

ered from Blake Escarpment are the oldest in-place rocks yet dredged from the floor of the deep Atlantic; they may even be older than the shallow reefal deposits of Lower Cretaceous age dredged from the Pacific guyots (13).

BRUCE C. HEEZEN

ROBERT E. SHERIDAN

Department of Geology and Lamont Geological Observatory, Columbia University, Palisades, New York 10964

#### References and Notes

1. B. C. Heezen, M. Tharp, M. Ewing, *The Floors of the Oceans* (Geol. Soc. Amer., New York, 1959); R. M. Pratt and B. C. Heezen, *Deep-Sea Res.* **11**, 721 (1964).
2. D. B. Ericson, M. Ewing, B. C. Heezen, *Amer. Assoc. Petrol. Geologists Bull.* **36**, 489 (1952); D. B. Ericson, M. Ewing, G. Wolin, B. C. Heezen, *Geol. Soc. Amer. Bull.* **72**, 193 (1961); A. R. Loeblich, Jr., and H. Tappan, *Micropaleontology* **7**, 257 (1961). The discovery in 1949 and subsequent exploration of the unconsolidated Tertiary and Upper Cretaceous sediments are reported, JOIDES drill hole No. 3 bottomed in Eocene 178 m below the sea floor, 90 km west of our hauls 3, 4, and 7; *Science* **150**, 709 (1965).
3. J. Ewing, M. Ewing, R. Leyden, *Amer. Assoc. Petrol. Geologists Bull.* **50**, 1948 (1966).
4. R. E. Sheridan, C. L. Drake, J. E. Nafe, J. Hennion, *ibid.*, p. 1972.
5. During a training cruise by Duke University's R.V. *Eastward*.
6. Each time the dredge bucket soon became snagged; in 12 instances, pulling at strains of 5500 to 6000 kg for from 10 minutes to 2 hours broke it free. Tension and "wire-out" were logged continuously. Wire angles on release were less than 5 degrees; wire-out (Table 1) closely approximated the true depth.
7. Unrefined velocity measurements, reliable to within 5 percent, were carried out on dry samples at room temperature and 1 atm pressure by a method similar to that of G. H. Sutton, H. Berckhemer, J. E. Nafe, *Geophysics* **22**, 779 (1957). The measured velocities compare favorably with those determined in nearby refraction profiles (4). A mixture of the 3.34-km/sec soft limestone and the dense 5.03-km/sec limestone of haul 7 might be observed seismically as a layer of intermediate velocity, similar to the 4.1-km/sec layer observed in refraction profiles.
8. Haul 4, taken in only slightly shallower water than haul 3, contained a fauna characterized by abundant miliolids and textularids, tentatively dated as Aptian, that is distinctly different from the Neocomian to Aptian fauna of haul 3.
9. P. L. Applin and E. R. Applin, *U.S. Geol. Surv. Profess. Paper* **447** (1965), 86 pp. The coarse bioclastic calcarenites, with algal fragments, found on Blake Escarpment resemble oil-reservoir rocks of southern Florida. The arch structures in the three deepest seismic horizons, along the eastern edge of Blake Plateau, may provide traps for any oil present.
10. N. D. Newell, *Nat. Hist.* **1959**(March), 119; **1959**(April), 227 (1959).
11. C. L. Drake, M. Ewing, G. H. Sutton, *Physics and Chemistry of the Earth* (Pergamon, London, 1959), vol. 3, pp. 110-98.
12. M. Ewing, T. Saito, J. I. Ewing, L. H. Burckle, *Science* **152**, 751 (1966); J. I. Ewing, J. L. Worzel, M. Ewing, *Trans. Amer. Geophys. Union* **47**, 122 (1966).
13. E. L. Hamilton, *Geol. Soc. Amer. Mem.* **64**, 97 (1956).
14. We thank Duke University Marine Laboratory for the use of R.V. *Eastward* on cruise E-9-66 in the Cooperative Oceanographic Program. This program, directed by R. J. Menzies, is supported through NSF grant G17669 to Duke University. The work at sea was greatly aided by Capt. R. Craig and Party Chief J. Cason, C. Bertelsen, J. Conally, D. Folger, P. J. Fox, H. Haring, T. Holcombe, M. Schneek, A. Lowrie, Jr., D. Needham, W. Ruddiman, and E. D. Schneider assisted at sea, N. K. Brown, Jr. (Esso Production Research Co.), S. F. Percival, Jr., L. Jones, K. Keller, L. R. Tucker (all of Mobil Oil Corp.), and T. Saito (Lamont Geological Observatory) assisted in stratigraphic paleontology. W. Ruddiman assisted in many ways both at sea and in the laboratory. A. McGarr assisted in measuring the compressional wave velocities. Report aided by grants from ONR (Nonr 266-48) and NSF (GA 580). Lamont Geological Observatory contribution 1009.

20 October 1966

## Garnet Zoning: An Interpretation Based on the Rayleigh Fractionation Model

**Abstract.** *Manganese zoning in almandine garnet is interpreted by the use of calculations based on the Rayleigh fractionation model. A close similarity of a measured manganese zoning profile and a calculated profile indicates that the assumptions used in the calculations are good. These assumptions are: complete removal of garnet from a homogeneous reservoir as the garnet crystallizes, and a nearly constant manganese fractionation factor between garnet and reservoir.*

Compositional zoning in almandine garnet, as measured with the electron microprobe, appears to be the rule rather than the exception; and it is most clearly characterized by decreasing Mn outward from the garnet center (1). This report offers a semiquantitative interpretation of zoning in garnets.

In a study of mineral growth histories and metamorphic reactions in the Kwoiek area of British Columbia 80 miles (130 km) northeast of Vancou-

ver (2), it was recognized that zoned almandine garnets are ubiquitous; Mn, Fe, and Mg zoning patterns of most of the garnets are similar to those shown in Figs. 1a and 1c. The Mn pattern of Fig. 1b is an exception, discussed below. The bell-like shape of the Mn profiles suggests that the cause of the zoning might be progressive depletion of Mn from the rock surrounding an individual garnet as the garnet grows. Because the garnet is zoned, successive layers are not in mutual

chemical equilibrium, and they cannot be in equilibrium with the rock external to the garnets. In fact, only the infinitesimally thin outer layer of the garnet can possibly be in equilibrium with the rest of the rock at any stage of garnet growth. The model proposed below is consistent with a concept of garnet growing from a reservoir of minerals which internally reequilibrate with changing conditions and which are therefore individually homogeneous.

Rayleigh (3) derived a mathematical expression for the composition of a liquid as it condensed and was continuously removed from a multicomponent vapor. This system is analogous to a garnet growing from a homogeneous reservoir and zoning as it grows. Neumann *et al.* (4) and McIntire (5) used a similar approach in considering the theoretical distribution of trace elements in crystals crystallizing from a magma as well as the concentration of trace elements in the magma during crystallization. Based on the basic method of Rayleigh (3), the following is a derivation of the formula used for the present work, which gives the weight percent of an element at the garnet edge as a function of the weight of garnet crystallized from the rock. The terms used are:

$M_G$  = weight fraction of element in garnet edge;

$W_M^R$  = weight of element in rock external to crystallized garnet;

$W_R$  = weight of rock external to garnet;

$M_R$  = weight fraction of element in rock excluding that in garnet;

$\lambda$  = fractionation factor,  $M_G/M_R$ ;

$W^0$  = initial weight of rock, prior to garnet crystallization;

$W_M^0$  = initial weight of element in rock, prior to garnet crystallization;

$M_0$  = initial weight fraction of element in rock, prior to garnet crystallization;

$W^G$  = total weight of crystallized garnet.

$$M_G = \frac{-dW_M^R}{-dW_R} \quad (1)$$

Equation 1 is a statement of the assumption of removal of garnet from the rock as the garnet crystallizes.

$$M_G = \lambda M_R = \lambda \frac{W_M^R}{W_R} \quad (2)$$

Equation 2 states that the weight fraction of Mn in garnet is proportional to that in the rest of the rock;  $\lambda$  may be an equilibrium fractionation factor

or it may be a steady-state fractionation factor. As each infinitesimal garnet layer grows, the immediately preceding layer has been effectively removed from the system so that the final system will have a composition differing from the initial composition of the system by the average weighted composition of the crystallized garnet, if garnet is the only zoned mineral in the rock.

Combining Eq. 1 and Eq. 2, and rearranging, gives

$$\lambda \frac{dW_R}{W_R} = \frac{dW_M^R}{W_M^R} \quad (3)$$

Integration, assuming  $\lambda$  a constant, gives

$$\lambda \ln \frac{W_R}{W^0} = \ln \frac{W_M^R}{W_M^0} \quad (4)$$

and

$$\lambda \ln \frac{W_R}{W^0} = \ln \frac{M_R W_R}{M_0 W^0} \quad (5)$$

$$\lambda \ln \frac{W_R}{W^0} = \ln \frac{M_R}{M_0} + \ln \frac{W_R}{W^0} \quad (6)$$

$$\ln \frac{M_R}{M_0} = (\lambda - 1) \ln \frac{W_R}{W^0} \quad (7)$$

$$\frac{M_R}{M_0} = \left( \frac{W_R}{W^0} \right)^{\lambda - 1} \quad (8)$$

By the use of Eq. 2 and

$$W_R = W^0 - W^G \quad (9)$$

The final equation is

$$M_G = \lambda M_0 \left( 1 - \frac{W^G}{W^0} \right)^{\lambda - 1} \quad (10)$$

Equation 10 gives the weight fraction of an element at the edge of a garnet in terms of  $M_0$ , the weight fraction of that element in the rock as a whole (including all that is in the crystallized garnet),  $W^G$ , the weight of the crystallized garnet,  $W^0$ , the weight of the original system, and  $\lambda$ , the fractionation factor between garnet and reservoir minerals, which is assumed a constant. However,  $\lambda$  can be a constant only if the element considered is minor enough that, for Mn as an example,  $Mn/(Mn+Fe+Mg) \approx Mn/(Fe+Mg)$ , for both garnet and reservoir minerals over the range of concentration involved. This assumption can be shown to hold for the range of Mn content observed in the garnet discussed below.

As a test of the Rayleigh depletion model, a rock specimen, referred to below as the type rock, was chosen for detailed study, which contained the following simplifying characteristics: (i) abundant garnet so that by comparison of several profiles, one could be chosen

which was from a thin section cut very near the garnet center; (ii) large enough grain size of the ferromagnesian minerals to insure accurate analysis of each mineral; (iii) negligible amounts of zoned ferromagnesian minerals other than garnet, to eliminate any complications that one zoned mineral might have on another; (iv) no microscopic evidence of retrograde effects; and (v) an assemblage with the maximum number of phases commonly observed to coexist in the Kwoiek area. The rock chosen had the following minerals and modal amounts: garnet, 4.1; biotite, 29.6; chlorite, 4.3; staurolite, 2.5; ilmenite, 1.0; graphite, 2.8; quartz and plagioclase (An 28-34, rims more sodic), 55.7; total, 100.

The relative amounts of quartz and plagioclase are not differentiated, because of the small grain size (0.02 mm) of these minerals in the type rock.

Both the garnet and staurolite are zoned, but the biotite and chlorite are unzoned. The biotite and chlorite must be unzoned and truly homogeneous in order to consider them as the reservoir during garnet growth in accordance with the model. Since the Mn counting rate for biotite and chlorite is close to the background counting rate, it is necessary to demonstrate that any zoning in Mn would be detectable. This was done by comparison with another sample with the same assemblage, but with higher Mn content in the garnet, from the same outcrop as the type rock.

Figure 1d shows the Mn profile of a biotite grain, measured across the cleavage, from the type rock. All biotite grains in the type rock had similar Mn counting rates and homogeneity (6). The biotite grains in the comparison rock were similarly homogeneous, but had a Mn counting rate three times greater. The Mn counting rate at the edge of the garnet in the comparison rock (see Fig. 1b) was as high as at the center of the garnet in the type rock (see Fig. 1a). Hence, if the biotite grains of the type rock were zoned and did not internally reequilibrate during garnet growth, the center of the Mn profile of Fig. 1d should have a counting rate three times that of the edge. As this is not the case, the biotite is homogeneous in contrast to the garnet. In addition, profiles of chlorite from both the type rock and the comparison rock demonstrate homogeneity.

We shall assume, in the application of Eq. 10 to Mn in the type rock,

that  $W^0$ , the weight of the system, is the sum of the weights of the minerals that exchange Fe and Mg with the garnet;  $M_0$  is, then, the weight fraction of Mn in the ferromagnesian minerals and not the rock as a whole. The ferromagnesian minerals in the type rock are biotite, chlorite, garnet, staurolite, and ilmenite. Most of the type rock's Mn content is now in the garnet. Biotite contains most of the remaining Mn. The contribution of ilmenite, staurolite, and chlorite is small because of their small amounts relative to biotite and their small manganese contents (0.3, 0.15, and 0.03 weight percent MnO, respectively).

In order to obtain  $M_G$  in terms of  $W^G/W^0$ , which can easily be put in terms of garnet radius,  $\lambda$  and  $M_0$  must be evaluated.  $M_0$ , which is the average weight percent of manganese in all the ferromagnesian minerals, was evaluated by determining the average content of each element in each mineral and weighting these numbers by the relative proportions of the minerals in the rock. The fractionation factor,  $\lambda$ , was evaluated by solving Eq. 10 for the center of the garnet where  $W^G/W^0 = 0$ .

Figure 2 shows the solution of Eq. 10, based on  $\lambda = 23$  as determined at the garnet center, compared with the measured values for the left half of the Mn profile of Fig. 1a.

The similarity of the two Mn curves is indicative that the assumptions made above, at least for Mn, are compatible with the data. The most important of these assumptions included in the basic Rayleigh equation is that as the garnet crystallized, its composition was removed from the system. Rayleigh's depletion model is, then, a convincing model for zoning of Mn in the garnet of the type specimen and, by inference, a convincing model for the Mn zoning of most garnet of the Kwoiek area.

The slight divergence of the calculated and measured curves may be explained in part by the fact that in determining the average weight percent of manganese in garnet a graphical integration technique was used on only one garnet. Separation of several garnets and measurement of the core compositions showed that the garnets were not of uniform size; furthermore, core compositions varied significantly, although the edge compositions were nearly constant. Thus, the average Mn content of the single garnet may not be a true average for the Mn content of all the garnets.

The divergence of the two curves could also be due to rising temperature during garnet growth. The fractionation factor calculated about 10  $\mu$  from the garnet edge was 14, which, being closer to 1 than 23 is, is in the expected direction for increasing temperature (7). However, other variables, in addition to pressure, that could affect the manganese fractionation factor may be (i) large deviations from the approximation that  $Mn/(Mn+Fe+Mg) \approx Mn/(Fe+Mg)$ , (ii) concentrations of other elements in any single phase of the assemblage, and (iii) relative proportions of the reservoir minerals. These possible variables can be understood by reference to Fig. 3. In this figure the edge Mn content of garnets from five rocks with the same assemblage, including the type specimen, collected from the same outcrop, is plotted against the Mn content of coexisting biotite and chlorite. Although there is

scatter in the points owing to low counting rates for Mn in biotite and chlorite and difficulties in the accurate analysis of the extreme edges of garnet, there are two distinctly different relationships for chlorite and for biotite. The slopes of the fitted lines are the fractionation factors between garnet and biotite and garnet and chlorite. The fractionation factor between garnet and the rest of the rock clearly depends on the relative proportions of biotite and chlorite. Both fractionation factors are greater than the 23 used for the calculation above, because of a sharp rise in Mn at the garnet edges, a phenomenon which probably involves effects on the fractionation factor as the rate of garnet growth approaches zero. The rise is only apparent on the right side of the Mn profile of Fig. 1a, but is more apparent in Fig. 1b. The assumption here is that the garnet in the five rocks stopped growing at about the same tem-

perature. Because the data of Fig. 3 suggest linear relationships, the fractionation factors cannot be highly dependent on concentrations of Mg or Fe over the range of data, as the concentrations of these elements differ between the garnets of the five rocks. This implies that Mn obeys Henry's law between the concentrations indicated on Fig. 3, which include the range of Mn concentration between center and edge of the garnet of the type specimen.

Changes in temperature and in the relative proportions of biotite and chlorite probably have the most important influence on the fractionation factor. During growth of the garnet, temperature might be expected to increase and the biotite/chlorite ratio would be expected to increase. However, estimates of the original biotite/chlorite ratio based on the mode of the type rock indicate that the effect

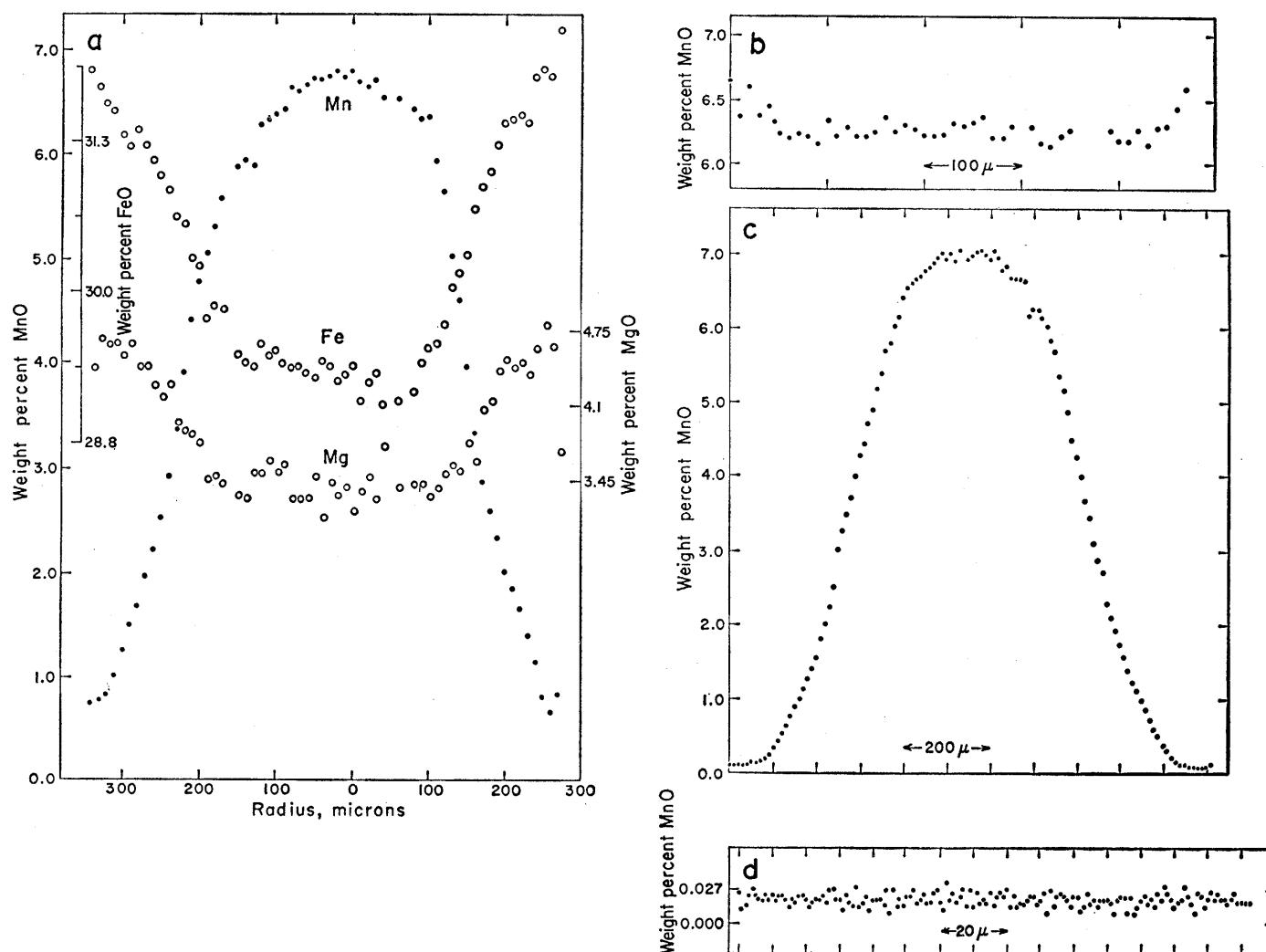


Fig. 1. (a) Mn, Fe, and Mg profiles across the type garnet. (b) Example of Mn profile of nearly homogeneous garnet. (c) Example of Mn profile across a garnet with edge Mn content approaching zero. (d) Mn profile across cleavage of a biotite grain from same rock as in (a). Electron microprobe analyses of (a), (b), and (c) spaced at 10- $\mu$  intervals; those of (d), at 1- $\mu$  intervals. Electron beam diameter for all analyses is less than 2  $\mu$ .

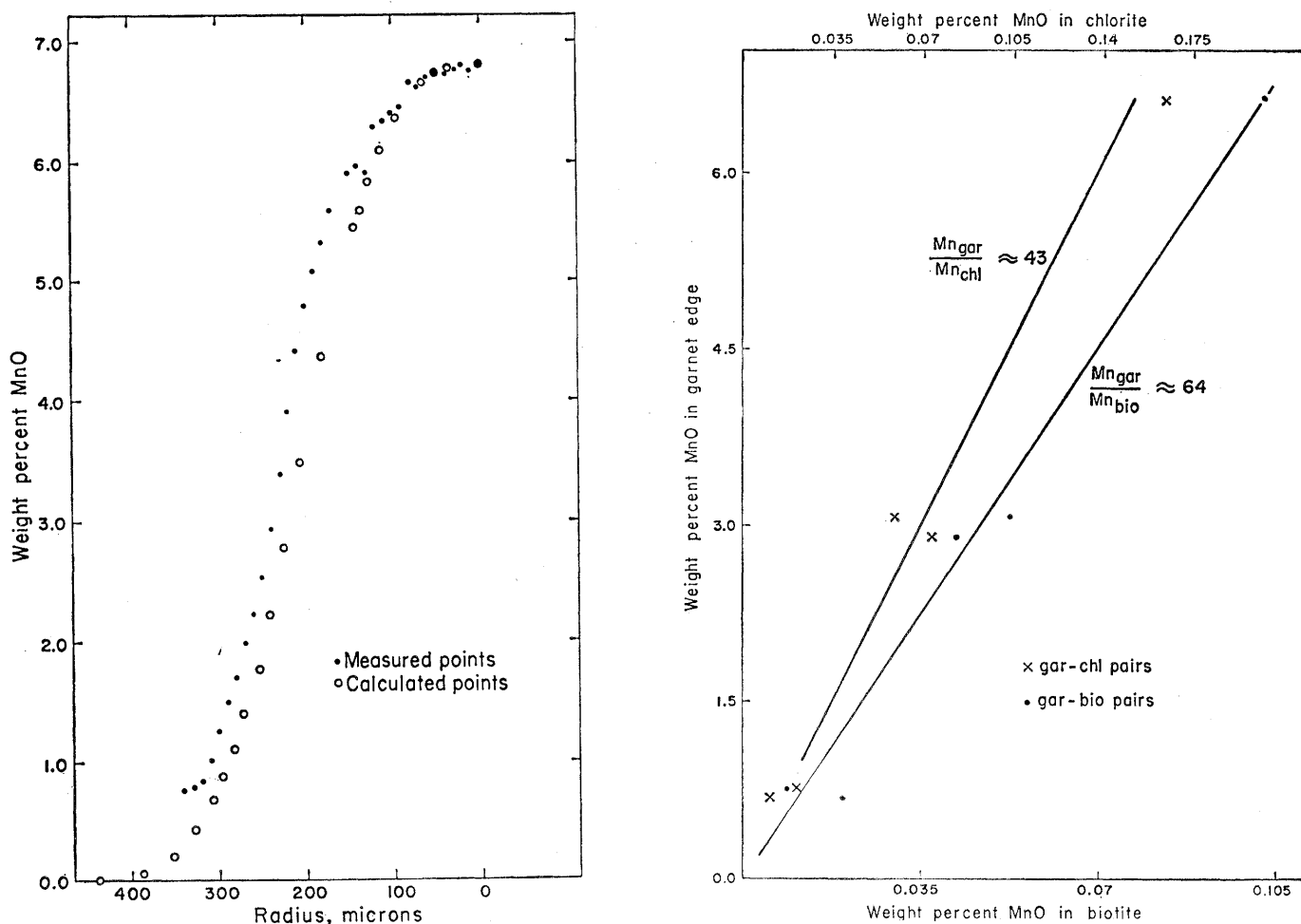


Fig. 2 (left). Comparison of left half of Mn profile of Fig. 1a (dots) with calculated profile (circles). Fig. 3 (right). Plot of edge content of Mn in garnet from five rocks with same assemblage from same outcrop against Mn content of coexisting chlorite (crosses and top scale) and biotite (dots and bottom scale).

of the changing biotite/chlorite ratio is not sufficient to account for the differences of the two curves of Fig. 2.

The very large Mn fractionation factor relative to the Mg and Fe fractionation factors can be considered the primary influence on garnet zoning. The fractionation factors for Mg and Fe between garnet and the rest of the rock are much less than for Mn: about 2 for Fe and 0.2 for Mg. As Mn in the rest of the rock is depleted, the Mn in the garnet necessarily drops, and, to maintain atomic balance in the garnet, Fe and Mg must increase as shown in Fig. 1a. If there were no Mn in the rock, the zoning in Fe and Mg in the garnet would be even less pronounced. Furthermore, unzoned garnets would be expected if the term  $W^G/W^0$  were near zero even at the end of garnet crystallization. Such a case has been observed (Fig. 1b) for the Mn profile of a single garnet in a thin section containing 34 percent biotite and chlorite.

If the garnet of Fig. 1a had continued to grow, the Mn content would

be expected to follow the calculated curve where it has been calculated beyond the existing garnet's edge. Garnets have been found in the Kwoiek area, with very small edge contents of Mn, which show Mn profiles similar to the calculated curve of Fig. 2. Figure 1c is one such example.

It can be concluded from this study that the model of Rayleigh depletion of Mn in the rock external to the garnet with lack of internal equilibration within the garnet is consistent with the analytic data of zoned almandine garnet. The necessary requirement of zoning is the large fractionation factor for Mn between garnet and the other Mn-bearing phases in the rock. It might also be expected that in certain situations calcium could also produce zoning. The behavior of calcium in the type garnet which shows an oscillatory zoning pattern between 2 and 2.6 weight percent CaO suggests that Rayleigh depletion does not totally describe the CaO variation, but garnets have been analyzed with Ca profiles similar to the

Mn profile of Fig. 1a, which suggests that in some assemblages depletion of CaO may be a major factor in the zoning of garnet. A petrologic consequence of zoning in minerals according to the model proposed is that the composition of the effective thermodynamic system of any assemblage would plot on a phase diagram in terms of the relative amounts of the homogeneous minerals, as the amount of the zoned minerals in the system is infinitesimally small.

LINCOLN S. HOLLISTER

Department of Geology, University of California, Los Angeles 90024

#### References and Notes

1. L. Hollister and A. Albee, *Geol. Soc. Amer. Abstr.* (1965); B. Evans, *ibid.* (1965); S. Banno, *Chishitsugaku Zasshi* **71**, 185 (1965); A. Albee, A. Chodos, L. Hollister, *Trans. Amer. Geophys. Union* **47**, 213 (1966); B. Harte and K. Henley, *Nature* **210**, 689 (1966).
2. L. Hollister, unpublished thesis, California Institute of Technology, Pasadena (1966).
3. L. Rayleigh, *Phil. Mag.* (6th series) **4**, 521 (1902).
4. H. Neumann, J. Mead, C. Vitaliano, *Geochim. Cosmochim. Acta* **6**, 90 (1954).
5. W. McIntire, *ibid.* **27**, 1209 (1963).
6. Differences in Mg/Fe ratio of biotite and

chlorite do exist between grains in different thin (0.5 mm thick) bedding laminae of the type rock, but these differences do not appear to be related to position relative to any garnet. Because of the low Mn counting rate, no systematic differences in biotite Mn content could be found. Each biotite had a Mn profile similar in magnitude to that of Fig. 1d. A gradient in Mn would affect the proposed model by affecting the fractionation factor.

7. A. Albee, *J. Petrol.* 6, 246 (1965).  
 8. I thank Dr. A. L. Albee, California Institute of Technology, Pasadena, for discussions, and A. L. Albee and Dr. W. G. Ernst, University of California, Los Angeles, for criticisms of the manuscript. Work supported by NSF grant gp-2773.

19 September 1966

## Level-Surface Profiles across the Puerto Rico Trench

*Abstract. Preliminary observations have been made from a ship of the warping of the geoid across the Puerto Rico Trench. Astrogeodetic and gravimetric measurements of the deflections of vertical and the corresponding level-surface profiles are compared for this site. The accuracies at which level-surface topography would provide a useful datum at sea are mentioned with reference to oceanographic requirements.*

Serial measurements of the deflections of vertical provide a means for tracing the posture of a level (equipotential) surface across reaches of ocean. Definition of an equipotential reference surface is fundamental to the study of ocean tides, changes of sea level, tilt of the sea surface due to wind stress, and if it is suitably refined, it serves as an origin for measuring the horizontal pressure gradients and geostrophic flow in ocean currents (1).

Deflections of the vertical were observed by direct (astrogeodetic) and verified by indirect (gravimetric) methods. The traverse was run from north to south along 66.3°W (Fig. 1) at a constant speed of 10 knots. The section started at 1000 (Q) on 31 March 1966 in 21.6°N over the ridge north of the Puerto Rico Trench, crossed the trench in a region where the free-air gravity anomaly is pronounced, and ended near San Juan, Puerto Rico at 0400 (Q) on 1 May 1966 as close to land as it was possible to bring the ship safely in darkness.

The site of this experiment enabled us to derive significant findings from relatively crude measurements. Where 66.5°W crosses the Puerto Rico Trench the free-air gravity anomaly approaches -385 milligal, and the anomaly isopleths are elongated in the east-west

direction. Thus, meridional deflections vertical of 1 minute of arc or more are to be expected, a magnitude which places them within the range of astrogeodetic measurement with available methods of marine navigation. Moreover, the trade winds in the area are usually steady and the ocean currents are generally weak and predominantly zonal, that is, running from east to west. These factors allow a single component experiment to be conducted in which the differences between geodetic and astronomical latitude can be compared with reasonable assurance that the zonal components of the deflection of vertical are small and that the local gradients of free-air gravity anomaly are predominantly meridional.

Astrogeodetic measurements of the deflections of vertical were made as the ship traversed the Puerto Rico Trench at constant heading and speed. Astronomical position was measured by GEON (2). Geodetic position was found by LORAN-A from stations 2L2 and 2L3.

The GEON system can indicate gravity vertical at sea with an r.m.s. (root mean square) error of 15 arc-sec. LORAN-A provides geodetic position with a far larger peak-to-peak error than 15 arc-sec; but in favorable weather and under constant speed and heading conditions, peak errors can be reduced by the method of running averages. This method was used, and it is expected that the r.m.s. error of the ship's position on the spheroid was found to an accuracy commensurate with that of the astronomical reckoning; the error was approximately  $\pm 0.2$  arc-min in each case.

Deflections of vertical,  $\xi$ , were computed according to the convention (3),  $\xi =$  astronomical latitude - geodetic latitude and with the assumption that deflections in the plane of the prime vertical were zero.

The short vertical lines in Fig. 2 show the departures of astronomical latitude from simultaneous fixes of the ship's position on the spheroid. The length of the strokes (0.4 arc-min) indicates the error in each comparison. The abscissa of each stroke indicates the geodetic latitude, and the ordinate, the sign of magnitude of the astronomical latitude or deflection of vertical.

Calculation of deflections of vertical and shape of the geoid from gravity data is a more complicated process. Stokes' theorem is considered to pro-

vide a means for computing the shape of the geoid from observed gravity anomalies, with the sole restriction that all disturbing masses lie inside the geoid, a condition that is well satisfied at sea. The theorem gives  $N$ , the normal distance from the geoid to the spheroid at a point  $P$ , as an integral function of free-air gravity anomalies,  $\Delta g$ ; namely,

$$N_P = \frac{a}{2\pi} \int_0^{2\pi} dA \int_0^\pi \Delta g f(\psi) \sin\psi d\psi$$

where  $a$  and  $g$  are mean values of the radius of the spheroid and the gravity upon it,  $A$  is the azimuth, and  $\psi$  is the angular distance from  $P$  to the gravity anomaly for the element concerned. But there is a difficulty in evaluating Stokes' formula in that the weighting function,  $f(\psi) \sin\psi$ , converges only very slowly to zero. As Garland (4) has put it: "The calculation of  $N$  at any point is in fact dependent on a knowledge of  $\Delta g$  over the whole earth, and even today there are barely sufficient observations in some regions to permit accurate calculations anywhere."

In an effort to avoid this difficulty, Heiskanen and Vening Meinesz (5) have shown that in a series expansion of the weighting function for the deflection of vertical, the first term is dominant for short distances—out to some 30 km from  $P$ . They also suggest that where the gradient of gravity anomaly is smooth, the azimuth of the near-field deflection of vertical will coincide with the direction of the gravity anomaly gradient.

The near-field formulas (5) for the north,  $\xi$ , and east,  $\eta$ , components of the deflection of vertical in the left-handed coordinate system are simply,

$$\delta\xi'' \simeq 0.105'' (\delta\Delta g/\delta y) r_0$$

and

$$\delta\eta'' \simeq 0.105'' (\delta\Delta g/\delta x) r_0$$

where  $\delta\Delta g/\delta y$  and  $\delta\Delta g/\delta x$  are the average free-air gravity anomaly gradients in milligals per kilometer across the north-south and east-west diameters, respectively, of a circle of radius  $0 < r_0 < 30$  km around a point  $P$ , within which gravity anomalies are accumulated.

Rice (6) has shown that the effect of increasing radius can be appreciable out to and sometimes beyond 200 km if accuracy of 1 arc-sec is required, and for values of  $r_0 = 30$  km or less only a major fraction of the total deflection may be accumulated (7). Thus